RSC Advances

ROYAL SOCIETY OF CHEMISTRY

www.rsc.org/advances

Journal Name

ARTICLE

Electrochemically prepared nanoporous gold as a SERS substrate with high enhancement

Cheng Fang,[a,†] Joseph George Shapter,[a] Nicolas Hans Voelcker[b] and Amanda Vera Ellis[a,*]

Single-molecule surface-enhanced Raman scattering (SM-SERS) utilizes localized surface plasmons in metallic nanostructures for enhanced signal detection. This work demonstrates the use of SM-SERS on an electrochemically anodized biocompatible nanoporous gold (NpAu) substrate using a bi-analyte Raman technique. It was found that the positions (so-called hot-spots) with the closest etched valley widths (w) or the smallest w/valley wall width (D) (ligaments) of the Au nanopores dominated the Raman scattering. By using an etched substrate with a $w < 10$ nm and a $w/D < 0.2$ an estimated enhancement factor of ~10^7 for both Nile blue and Rhodamine 6G dyes was achieved. Importantly, the bi-analyte Raman technique enabled the clear confirmation of single (or few) molecule detection on the Np/Au substrates.

1. Introduction

Surface-enhance Raman scattering (SERS) has received increasing attention due to its enhanced signal-to-noise ratio and high sensitivity (down to single molecule detection (SMD)).[1-3] It is well-known that there are two kinds of signal enhancement namely, electromagnetic and chemical enhancement, although the detailed mechanism of these still remains unclear.[3, 4] The former, and most widely agreed upon, originates from nano-sized structures on the substrate surface. In this case enhanced Raman scattering dominates when the electro-magnetic field from the nanostructure is extremely high, and these locations are often referred to as hot-spots.[5, 6] Therefore development of substrates with controllable nanostructures, and thus hot-spots, is highly attractive however still remains a challenge.

To date there have been many types of SERS substrates fabricated, including roughened metal surfaces,[7] nanoparticle arrays,[5] nanofabricated surfaces[8] and nanoaggregates.[9, 10] Nanostructuring and nanoaggregates have recently shown the most promise as more precise control over the hot-spots can be achieved.[11] Organised dimers and trimers of silver and gold nanoparticles have been used to identify hot-spot positions.[6, 12] While complex flower-like structures of silver[11] and gold,[13] nanotriangles[14] and nanowires[4] have been used to replace nanoparticles in an attempt to obtain an anisotropic signal or to identify the position of the hot-spot. In an attempt to create large scale SERS substrates a lithography technique[1, 8] has been used whereby periodic structures extending over areas greater than ~1 mm^2 were produced on various templates, including porous silicon and aluminium.[15, 16] A less time-consuming approach has been the fabrication of nanoporous gold (NpAu), which can be produced on large scales (~1 cm^2)

with high stability.[17-20] However, fabrication of NpAu SERS substrates with controllable feature sizes (hot-spots) has proven to be difficult.[17] Many researchers have used a de-alloying approach to produce NpAu substrates however mandatory post annealing in order to facilitate pore size tuning resulted in a lower Raman enhancement and thus reduced SERS response.[18, 21, 22]

A more promising technique to control pore size in NpAu substrates is electrochemical pore-etching.[23-25] However, the challenge here is that the electrochemical etching on noble metals is not as well-established as pore-etching on semiconductors. The reason for this is that there is a space-charge layer on semiconductors which does to exist on noble metals. This means that the etching current is difficult to focus for controllable pore etching. Recently, we have shown that electrochemical pore-etching on noble metals (silver and gold) is possible by carefully selecting the etching solutions (an HF-based organic electrolyte), and current densities.[26, 27]

This work shows the fabrication of NpAu SERS substrates with tuneable pore sizes using electrochemical etching of an ~300 nm gold film on a silicon substrate in hydrofluoric acid (HF) and N,N- dimethylformamide (DMF) (1:1 v/v). We then studied the effect of pore size, valleys and ligaments of the NpAu substrates on the Raman enhancement of Rhodamine B, Rhodamine 6G (R6G) and Nile blue (NB) dyes in order to develop an effective SERS substrate with high reproducibility and stability.

2. Experimental section

2.1. Chemicals

All chemicals including Rhodamine B (RB), Rhodamine 6G (R6G) and Nile blue (NB) were purchased from Sigma–Aldrich (Australia) and used as supplied. The etching solution was formulated using a volume ratio (1:1 v/v) of aqueous HF (48 %) and analytical grade DMF.

2.2. NpAu Fabrication

A gold film of ~300 nm thickness was sputter coated onto a silicon wafer at the Australian National Fabrication Facility (ANFF, Brisbane, Australia). This gold coated substrate was then cleaned with fresh Piranha solution (70:30 v/v concentrated sulfuric acid:hydrogen peroxide) for 2-3 min (*Be careful: this solution will react vigorously with organic materials!*). After which the substrate was washed with copious amounts of Milli-Q water (18.2 MΩ.cm) and dried under a stream of nitrogen gas.

Electrochemical etching of the gold film to produce the NpAu substrates was carried out at an anodization potential ramped from 0 V to 5 V over 20 s and 30 s; 0 to 10 V over 20 s and 30 s; 0 V to 20 V over 30 s; 0 V to 40 V for 30 s using a Keithley 2612 System SourceMeter® controlled by Lab-view software.[26, 27] The anodization potential was also held at 20 V for 10 s and 30 s; and 40 V for 60 s. Two kinds of electrochemical cells were used for the anodization (see, Figure 1 and 2). The etching solution was either stirred to accelerate the transportation of reactants and products for a 3-electrode configuration of etching cell (Fig. 1(a)) or kept static to stabilize the diffusion layer for a 2-electrode configuration (Fig. 2(a)). The typical dependence of current on the potential (*i-V* curves) (Fig.1(b) and 2(b)) show their anode polarization process. More details can be seen in Refs. 26 and 27.

2.3. Substrate characterization and SERS detection

In order to characterize the nanoscale surface topography of the NpAu SERS substrates focussed ion beam/scanning electron microscopy (FIB/SEM) was carried out using a Helios D433, Dual Beam FiB/SEM, FEI Co., USA.

Evaluation of the Raman enhancement of the NpAu SERS substrates was achieved using RB, R6G and NB dyes as Raman
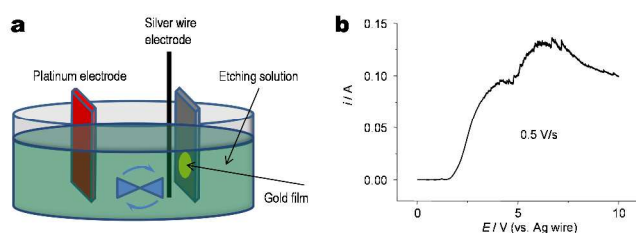

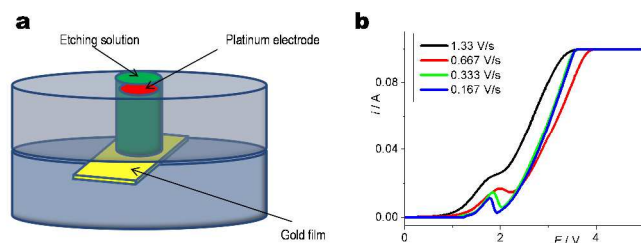Fig. 1. Etching cell of three-electrode configuration (a) and its *i-V* curves (b).

Fig. 2. Etching cell of two-electrode configuration (a) and its *i-V* curves (b).

probes. All NpAu SERS substrates were incubated for approximately 3 h in an aqueous solution of RB (1×10^{-9} M), R6G (2×10^{-9} M) or NB (1×10^{-8} M) with NaCl (1 mM). After 3 h the substrates were removed and washed with Milli-Q water and dried under a stream of nitrogen.

All Raman spectra were collected in air using a Witec Confocal Raman Microscope (Alpha 300RS, Germany) equipped with a 532 nm laser diode (< 60 mW). A CCD detector (cooled to ~−60 °C) was used to collect Stokes Raman signals under a × 40 objective (Nikon) at room temperature (~24 °C) in a wavenumber range of 0–2000 cm⁻¹ with an integration time of 5 s for each measurement. By tuning the laser intensity to balance between the Raman signal intensity and stability no significant decline in the Raman intensity was observed that would otherwise arise from the thermo-effect within this integration period.[28]

2.4. Bi-analyte Raman scattering spectroscopy

In order to evaluate the efficiency of the nanoporous SERS substrate and to confirm SMD, a bi-analyte Raman experiment was performed.[29-32] A NpAu substrate (etched at 40 V for 60 s in a 2-electrode static cell (Fig. 2)) was incubated in an aqueous solution of R6G (2×10^{-9} M) and NB (1×10^{-8} M) in the presence of NaCl (1 mM) for ~3 h. The substrate was then removed and washed with Milli-Q water and dried under a stream of nitrogen.

For bi-analyte Raman analysis the NpAu SERS substrate was scanned with a 532 nm laser diode (< 60 mW) over an area of 80 μm × 80 μm with a pixel array of 50 × 50 while the Raman signal was collected using a ×100 objective (Nikon). The integration time was 0.1 s for each pixel of signal collection. The mapping image was generated based on the intensity of their main characteristic peaks, which were at ~613 cm⁻¹ for R6G and ~590 cm⁻¹ for NB, respectively. Again, the minimum intensity of laser (whilst a collectable Raman signal) was used to avoid the thermo-effect.[28,33]

3. Results and discussion

Fig. 3 (a−d) shows the surface topographies of NpAu SERS substrates after etching a gold film (approximately 300 nm on a Si substrate) in a 3-electrode stirred cell (Fig. 1). The figures clearly show the appearance of valleys and valley walls (ligaments) resulting in a nanoporous gold film. Fig. 3 (a) shows the etched surface after a ramped potential is applied from 0 V to 20 V over 30 s (0.67 V/s), indicating many etched valleys (see arrows). The width (*w*) of the etched valleys in Fig. 3(a) are 5−15 nm (a statistical average of ~10 measurements). When the ramped potential was reduced from 0 V to 10 V over 20 s (0.5 V/s) (Fig. 3(b)) there was an increase in *w* from 5−15 nm to 20−40 nm, originating from the merging of neighbouring pores during the etching process.[27] When the voltage was held at 20 V for 20 s and 30 s, see Fig. 3 (c and d) respectively, the *w* also increased to 40−60 nm.

Fig. 3 (e) shows the corresponding depths for each etch (Fig. 3 (a-d) are shown in also increase from 80−100 nm (Fig. 3 (a and b)) to 120−150 nm (Fig. 3 (c)) to approximately 250 nm (Fig. 3 (d)), a result of controlling the etching period.

These NPAu SERS substrates were then incubated in aqueous RB solution (1×10^{-9} M) in order to study the nanostructure contribution to SERS enhancement. Figure 3 (f) shows the Raman signals collected from each respective surface. The background signal stems from the nano-size

gold.[27] The SERS response (peak height at 1653 cm^{-1}) was strongest from the surface presented in Fig. 3 (a). That is, the Raman scattering is strong when w is less than 15 nm. This is an important consideration because when w is small the electromagnetic field from neighbouring valley walls (ligaments) can overlap and couple, thus significantly enhancing the Raman scattering effect.[17-20]

The surface shown in Fig. 3 (a) shows the greatest enhancement, however, has the lowest pore depth penetration (<100 nm) in comparison to the other etching profiles. This suggests that the etching depth has little effect on the signal enhancement and that enhancement is predominately from the top surface edge states of the pores. This is true even though the laser penetration depth is approximately ~20 μm.[6] An additional factor that affects the electromagnetic field is the width of the ligament (valley wall) (D), which varies from 30−40 nm (Fig. 3 (a)) to 50−60 nm (Fig. 3 (b)) to 40−50 nm (Fig. 3 (c and d). In an electrochemical process the ability to tune D gives a distinct advantage in comparison to a de-alloying approach, where the pore with is always approximately equal to the ligament width.[20]

Fig. 3 (f) shows that the nanostructure with the smallest w and w/D (hot-spot positions) features (Fig. 3 (a)) have the strongest electromagnetic field, thus dominating the collected Raman signal.[13, 16]

In an attempt to obtain a higher SERS enhancement and quantitative Raman signals the RB concentration was increased from 1×10^{-9} M to 1×10^{-8} M. In addition, the w was decreased by keeping the etching solution static in a 2-electrode cell (Fig. 2) and the etching conditions were optimized to increase the nucleation density.[26, 27] Figure 4 shows the topographies of the etched gold film.

The etching was carried out in a static solution of 1:1 (v/v) HF:DMF at a ramped potential from 0 V to 5 V for 30 s (Fig. 4 (a)); or from 0 V to 10 V for 30 s (Fig. 4 (b)); or from 0 V to 40 V for 30 s (Fig. 4 (c)); or at 40 V for 60 s (Figure 4 (d)). The etching in Fig. 4 (a) is shallow and the surface is roughened. With the increased ramping slope of the polarization potential from 5 V (Fig. 4 (a)) to 10 V (Fig. 4 (b)) and 40 V (Fig. 4 (c)), the etching develops into pronounced valleys.

When the potential was kept constant at 40 V (Fig. 4 (d)) the etching nucleation density was much higher than when a ramping potential was applied to the surface (Fig. 4 (a-c)), indicated by non-uniform nanostructures on the surface.

Fig. 4 (e) shows the Raman signals collected from the NpAu SERS substrates (Fig. 4 (a-d)). Here, the intensities are observed to increase with the substrate produced at 40 V for 60 s showing the strongest Raman response (Fig. 4 (d)). This substrate has the smallest w at approximately 2 nm, further indicating the importance of the nanostructure in the formation of hot-spots.[1, 2, 18]

Fig. 4 (f) shows 10 spectra collected randomly across the surface shown in Fig. 4 (d) where the signal is shown to be repeatable. As with the previous data the background signal stems from the nano-size gold.[27]

Fig. 5 (a) and (b) shows the dependence of the Raman intensity on w and w/D, respectively from the surfaces in Fig. 4 (a-d). It can be seen that an extremely strong enhancement originates when w is ~2 nm and w/D is ~0.1. This supports the hypothesis that large ligament widths contribute to signal enhancement. These results are encouraging and confirm the prediction that the w and w/D effect the Raman enhancement, indicating the benefits of employing electrochemically etched NpAu as SERS substrates rather than de-alloyed metal where the ligament width is not so readily tuneable.

In order to confirm single molecule Raman scattering, a bi-analyte Raman experiment was carried out.[29-32] In this case when sufficiently low concentrations of both analyte molecules were introduced onto the NpAu substrate, on average, only one type of molecule is adsorbed to each hot spot. Therefore, each SERS spectrum contains spectral features of only a single molecule. On the other hand, as the coverage is increased such that both analytes should be present on a single spot, the vibrational characteristics of both analytes can be observed. Thus, this technique can distinguish single- versus multi-molecule SERS by the number of peaks in the SERS spectrum.

In order to undertake this experiment a NpAu SERS substrate, the topography of which is shown in Fig. 3 (d) was incubated at room temperature in a solution containing both NB (1×10^{-8} M) and R6G (2×10^{-9} M) dyes.
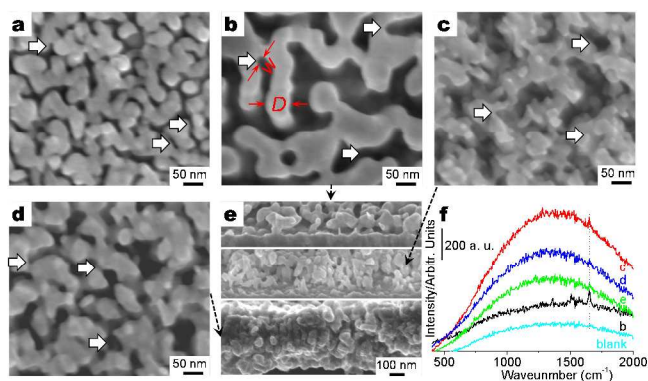

Fig. 3. Typical FIB/SEM images of gold substrates electrochemically etched in a 3-electrode stirred cell a solution of HF:DMF 1:1 (v/v) at (a) a ramped potential from 0 V to 20 V over 30 s, (b) a ramped potential from 0 V to 10 V over 20 s, (c) at 20 V for 10 s and (d) at 20 V for 30 s. (e) shows the cross sectional view of images (b−d) from top to bottom, respectively. (f) shows the typical SERS response of each of these surfaces (blank before etching and (a−d) after etching) using RB at 1×10^{-9} M. D and w are indicated in (b) as an example.
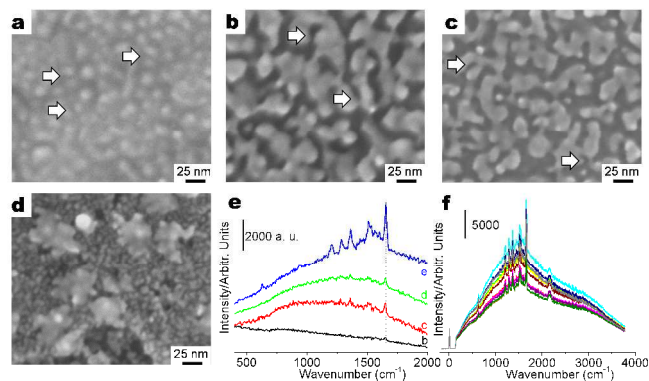

Fig. 4. Typical FIB/SEM images (a−d) of gold substrates electrochemically etched in a 2-electrode static cell with a solution of 1:1 (v/v) HF:DMF at (a) a ramped potential from 0 V to 5 V for 30 s, or (b) from 0 V to 10 V for 30 s , (c) from 0 V to 40 V for 30 s, (d) at 40 V for 60 s, respectively and (e, f) SERS response of NpAu substrates using RB (1×10^{-8} M with 1 mM NaCl) as a Raman probe. The spectra in (f) were 10 spectra collected randomly over the surface of (d).
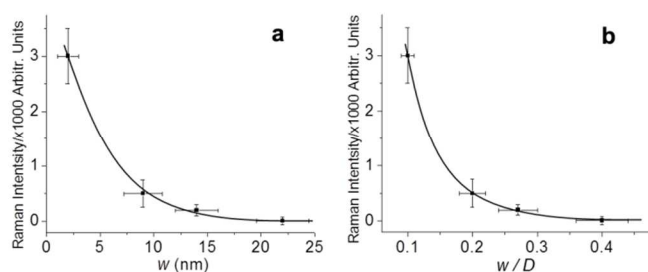
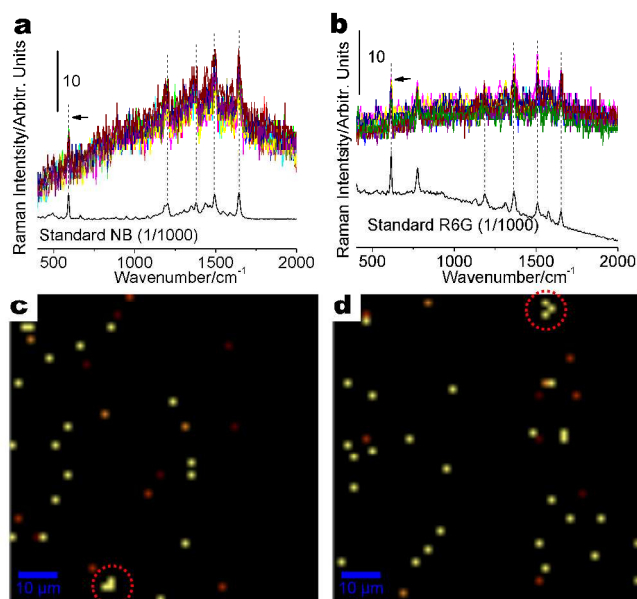Fig. 5. SERS intensity dependence on (a) *w* and on (b) *w/D*.

Fig. 6. SERS response of bi-analyte Raman probes. (a and b, top) show the average spectra of pure NB and R6G dyes collected individually from the same scanning area (~80 × 80 μm²) on a NpAu SERS substrate, (a and b, bottom) shows the typical spectra of NB and R6G dyes for comparison and (c and d) shows the mapping images (~80 × 80 μm²) based on selected characteristic peaks at ~589 cm⁻¹ for NB and ~613 cm⁻¹ for R6G. The solution containing 2×10^{-9} M R6G, 1×10^{-8} M NB and 1×10^{-3} M NaCl was used for incubation.

These concentrations were chosen as they are associated with the dyes' respective limits of detection, considering a signal/noise ratio (>3)). The substrate contain nanostructure features of w <10 nm and w/D <0.2.

Fig. 6 (a) and (b) top shows the Raman spectra acquired on the NpAu SERS substrate for the NB and R6G dyes, respectively while the spectra shown with the lowest intensity in Fig. 6 (a) and (b) are the typical individual reference spectra for the NB and R6G dyes, respectively. Raman mapping images of the NB and R6G dyes are shown in Fig. 6 (c) and (d), respectively. These maps are based on the Raman scattering intensity of the characteristic peaks at ~589 cm⁻¹ for NB (Fig. 6(a, c) and R6G and ~613 cm⁻¹ for R6G (Fig. 6(b, d)). Depending on the peak intensity, a dot in the mapping images was brightened (from red, to orange then to yellow; representing increasing Raman intensity). The dark background implies no detectable Raman scattering form the dye.

The bright dots in Fig. 6 (c and d) correspond to the so-called hot-spot positions. Pure signals from either NB or R6G are observed frequently because there is almost no overlapping of the bright dots (< 5%) (as observed inside the dotted circles in Fig. 6 (c and d)). Consequently the appearance of predominately single molecule signals suggests that the hot-spots are mainly occupied only by either one NB molecule (Fig. 6 (c)) or one R6G molecule (Figure 6 (d)), or only one molecule (NB or R6G) dominates the Raman scattering within a signal collection period (0.1 s) from one pixel. In other words, single molecule detection is achieved.

Standard spectra were also collected from bulk powder samples of NB and R6G (see Fig. 6 (a) and (b) , respectively) under similar laser intensity and integration times to estimate the enhancement factor (*EF*) as per the following equation: [1, 2]

$$EF = [I_{SERS}/N_{SERS}] / [I_{powder}/N_{powder}]$$

where I_{SERS} is the intensity of SERS signal, N_{SERS} the number of molecules involved. I_{powder} and N_{powder} are the corresponding parameters for a powdered sample. Taking the laser spot size as 1−2 μm² and its penetration depth as approximately 20 μm,[6] a laser spot can cover approximately 10^{-10} g sample (if the density of the dye (N_{powder}) is around 3 g/cm³). This is approximately 3×10^{-13} moles, according to a molecular weight of approximately 400 g/mol or approximately 2×10^{11} molecules of powder (N_{powder}). Thus from Fig. 6 (a and b) the enhancement factor for a single molecule ($N_{SERS} = 1$) of NB or R6G was thus estimated to be ~10⁷ by comparing the Raman intensity of their characteristic peaks (I_{SERS} versus. I_{powder}).

4. Conclusions

Here we demonstrate the size-controllable electrochemical etching of gold films in HF/DMF solution to produce NpAu SERS substrates. These were shown to successfully act as a SERS substrate in the analysis of NB and RB dyes. Importantly, the positions (so-called hot-spots) with the closet *w* or the smallest *w/D* (rather than the statistical or average value) dominate the Raman scattering. An estimated enhancement factor of ~10⁷ for both NB and R6G dyes was observed with good uniformity across the substrate when the nanostructure features of *w* were <10 nm and *w/D* was <0.2. The simultaneous use of the bi-analyte Raman technique enabled a clear confirmation of the single (or few) molecule nature of the signals. These substrates offer the potential to act as stable Au SERS substrates for real-world applications.

Notes and references

[a]Flinders Centre for Nanoscale Science and Technology, School of Chemical and Physical Sciences, Flinders University, Sturt Road, Bedford Park, Adelaide SA5042, Australia. E-mail: amanda.ellis@flinders.edu.au.

RSC Advances Accepted Manuscript

[b]Mawson Institute, University of South Australia, Mawson Lakes, Adelaide 5095, S.A., Australia.
†Current address: CERAR, University of South Australia, Mawson Lakes, Adelaide 5095, S.A., Australia. E-mail: cheng.fang@unisa.edu.au.

1   P. L. Stiles, J. A. Dieringer, N. C. Shah and R. P. van Duyne, *Annu. Rev. Anal. Chem.*, 2008, **1**. 601.
2   C. L. Haynes, A. D. McFarland and R. P. van Duyne, *Anal. Chem.*, 2005, **77**, 338A.
3   L. Tong, T. Zhu, Z. Liu, *Chem. Soc. Rev.,* 2011, **40,** 1296.
4   T. Chen, H. Wang, G. Chen, Y. Wang, Y. H. Feng, W. S. Teo, T. Wu, and H. Y. Chen, *ACS Nano*, 2010, **4**, 3087.
5   W.E. Doering and S. Nie, *J. Phys. Chem. B*., 2002, **106**, 311.
6   K. L. Wustholz, A. I. Henry, J. M. McMahon, R. G. Freeman, N. Valley, M. E. Piotti, M. J. Natan, G. C. Schatz, R. P. Van Duyne, *J. Am. Chem. Soc.,* 2010, **132**, 10903.
7   K. -H. Yang, Y. -C. Liu, and C. -C. Yu, *Langmuir* 2010, **26**, 11512.
8   C. Fang, A. Agarwal, K. D. Buddharaju, N. M. Khalid, S. M. Salim, E. Widjaja, M. V. Garland, N. Balasubramanian and D. -L. Kwong, *Biosens. Bioelectron.*, 2008, **24**, 216.
9   M. J. Mulvihill, X. Y. Ling, J. Henzie and P. Yang, *J. Am. Chem. Soc.,* 2010, **132**, 268.
10 S. Y. Lee, L. Hung, G. S. Lang, J. E. Cornett, I. D. Mayergoyz, O. Rabin, *ACS Nano,* 2010, **4**. 5763.
11 J. H. Bang and K. S. Suslick, *Adv. Mater.*, 2009, **21**, 1-5.
12 I. A. Larmour, K. Faulds, D. Graham, J. *Phys. Chem. C*, 2010, **114**, 13249.
13 G. Duan, W. Cai, Y. Luo, Z. Li and Y. Li, *Appl. Phys. Lett*., 2006, **89**, 211905.
14 K. P. Browne, B. Kowalczyk, B. A. Grzybowski, *Angew. Chem. Int. Ed*., 2010, **49**, 6760.
15 Y. Jiao, D. S. Koktysh, N. Phambu, and S. M. Weiss, *Appl. Phys. Lett.*, 2010, **97**, 153125.
16 H. -H. Wang, C. -Y. Liu, S. -B. Wu, N. -W. Liu, C. -Y. Peng, T. -H. Chan, C. -F. Hsu, J. -K. Wang and Y. -L. Wang, *Adv. Mater.*, 2006, **18**, 491.
17 S. O. Kucheyev, J. R. Hayes, J. Biener, T. Huser, C. E. Talley and A. V. Hamza, *Appl. Phys. Lett.*, 2006, **89**, 053102.
18 L. H. Qian, X. Q. Yan, T. Fujita, A. Inoue and M. W. Chen, *Appl. Phys. Lett.*, 2007, **90**, 153120.
19 L. H. Qian, A. Inoue, M. W. Chen, *Appl. Phys. Lett.*, 2008, **92**, 093113.
20 X. Y. Lang, L. Y. Chen, P. F. Guan, T. Fujita and M. W. Chen, *Appl. Phys. Lett.*, 2009, **94**, 213109.
21 J. Erlebacher, M. J. Aziz., A. Karma, N. Dimitrov and K. Sieradzkl, *Nature*, 2001, **140**, 450.
22 T. Fujita, L. -H. Qian, K. Inoke, J. Erlebacher and M. -W. Chen, *Appl. Phys. Lett.,* 2008, **92**, 251902.
23 Y. L. Khung, N. H. Voelcker, *Optical Materials*. 2009, **32**, 234-242.
24 A. Jane, R. V. Dronov, A. Hodges and N. H. Voelcker, *Trends in Biotechnology*, 2009, **27**, 230.
25 C. Fang, H. Foell, J. Carstensen, *Electroanal. Chem.*, 2006, **589**, 259.
26 C. Fang, A. V. Ellis, N. H. Voelcker, *J Electroanal. Chem.*, 2011, **659**, 151.
27 C. Fang, M. B. Narasimha, A. V. Ellis, N. H. Voelcker*, J Mater. Chem*., 2012, **22**, 2952.
28 M. Roca, A. J. Haes, *J. Am. Chem. Soc.*, 2008, **130,** 14273.
29 P. G. Etchegoin, E. C. Le Ru, *Anal. Chem.,* 2010, **82**, 2888.
30 P. G. Etchegoin, E. C. Le Ru, A. Fainstein, *PCCP*, 2011, **13**, 4500.
31 J. E. Bohn, E. C. Le Ru, P. G. Etchegoin, *J. Phys. Chem. C*, 2010. **114,** 7330.
32 E. C. Le Ru, M. Meyer, P. G, Etchegoin, *J. Phys. Chem. B*, 2006, **110**, 1944.
33 W. Zhang, T. Schmid, B. Yeo, R. Zenobi, *J. Phys. Chem. C*, 2008, **112**, 2104

Gold films were electrochemically etched into nanoporous substrates with tuneable pore sizes down to approximately 2 nm. The SERS enhancement as a result of changes in valley and ligament widths of the nanoporous gold was investigated. Compared to the conventional de-alloyed nano-gold, the etched gold showed a lower limit of detection (2×10^{-9} M *vs* 1×10^{-7} M Rhodamine 6G). Using a bi-analyte technique single molecule detection was achieved.
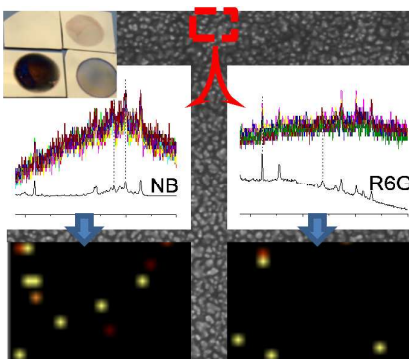
Single-Molecule Surface-Enhanced Raman Scattering on Electrochemically Prepared Nanoporous Gold Cheng Fang, Joseph George Shapter, Nicolas Hans Voelcker, and Amanda Vera Ellis*